

# Assessing ocean-model sensitivity to wind forcing uncertainties

I. Andreu Burillo,<sup>1</sup> G. Caniaux,<sup>1</sup> M. Gavart,<sup>2</sup> P. De Mey,<sup>3</sup> and R. Baraille<sup>2</sup>

Received 28 November 2001; accepted 4 March 2002; published 18 September 2002.

[1] In this paper, we assess the short-term forecast error of a mesoscale primitive-equation open-ocean model, induced by uncertainties in wind forcing. Statistics calculated from an ensemble of ocean states show that temperature forecast error is strongest at the top of the ensemble-mean thermocline, as a consequence of vertical displacement of the mixed-layer base around its ensemble mean. Horizontal pattern of the temperature error in the mixed-layer is mainly explained by horizontal advection and surface heat flux fluctuations. These two mechanisms and entrainment through the mixed-layer bottom are presented as the three processes responsible for thermal forecast error growth in the modeled upper ocean.

**INDEX TERMS:** 4572 Oceanography: Physical: Upper ocean processes; 4504 Oceanography: Physical: Air/sea interactions (0312); 4263 Oceanography: General: Ocean prediction; 4524 Oceanography: Physical: Fine structure and microstructure. **Citation:** Burillo, I. A., G. Caniaux, M. Gavart, P. De Mey, and R. Baraille, Assessing ocean-model sensitivity to wind forcing uncertainties, *Geophys. Res. Lett.*, 29(18), 1858, doi:10.1029/2001GL014473, 2002.

## 1. Introduction

[2] Casting the ocean is subject to errors due to initialization, forcings and parameterization of physical processes. Numerical artefacts, as for instance, open boundaries, are an additional source of error.

[3] Surface fluxes provide a model upper boundary condition. Consequently, they have a significant impact on the forecast. However, air-sea fluxes are yet affected by uncertainties, especially at low and strong winds. Parameterization and calibration of heat, momentum and mass exchanges between ocean and atmosphere are limited by measurement inaccuracies. Moreover, the implication of both atmospheric and oceanic spatial and time scales, points out the question of how these fluxes should be cumulated in time and aggregated on model grids and what would the effect of this treatment be upon model forecast.

[4] Air-sea exchanges have become, for this reason, a main subject in operational and research oceanography, with an increasing number of programmes of which some of the most recent are AUTOFLUX [Larsen *et al.*, 2000], SEA-FLUX [Fairall *et al.*, 2001] and ALBATROS [Weill *et al.*, 2002], dedicated to the different aspects mentioned above.

[5] Forcing an ocean model with inconsistent fluxes results in a misleading thermal content of the upper ocean, bringing the (forced or coupled) system to diverge.

[6] The object of this study, is to explore the influence of wind-induced uncertainties in air-sea fluxes upon upper ocean forecast, at short-time scales (of the order of a few days). In that purpose, we used an ensemble approach, as in Echevin *et al.* [2000].

## 2. The Model

[7] The model used is a regional version of the OGCM OPA8 [Madec *et al.*, 1997] having time-evolving open boundaries and a recirculation area [Gavart *et al.*, 1999] that assures transport conservation. The grid is 10 km in the horizontal. In the vertical, it stretches from 5m at the top layers to 170 m between the last two levels. An embedded 1.5 turbulence closure scheme represents mixed layer processes.

[8] Model is configured using data issued from the Intensive Observation Period (IOP) of the SEMAPHORE experiment [Eymard *et al.*, 1997], which took place in the Azores-Madeira region from 20/10/93 to 11/11/93. The region is characterized by a meandering front (the *Azores Front*, Figure 1) that separates relatively warm and salty waters in the south-western part of the domain, from fresher and colder waters in the north-eastern part of the domain. To this front is associated the *Azores Current*. Observed mixed-layer depths for the period simulated, vary from side to side of the frontal system, with values around 80 m in the warmer waters and shallower thickness of the order of 40 m in the northern part of the domain.

[9] The use of temperature and salinity analyses [Caniaux and Planton, 1998] for initial and lateral boundary conditions, limits the depth of the modeled domain to 2000 m, the bottom being considered flat (we believe this not to be a major limitation in the validity of our results). Radiative fluxes are provided by CMS (Centre de Météorologie Spatiale - Météo-France) in Lannion. Momentum and SST-dependent heat turbulent fluxes are computed via Large and Pond [1981, 1982] parameterizations.

[10] The SEMAPHORE IOP took place during the mixed-layer deepening season. During the second week of the IOP, a storm taking place in the vicinity of the domain from 29/10/93 until 31/10/93 brought strong north-westerly winds to the region, increasing stirring within the upper ocean. This resulted in increased mixed-layer cooling and deepening, associated to strong heat fluxes and entrainment at the mixed-layer bottom.

[11] The model successfully reproduces the characteristics of the frontal system [Caniaux and Planton, 1998; Gavart *et al.*, 1999], as well as mixed-layer deepening.

## 3. The Method

[12] A collection of 100 simulations was run for a seven-day period, corresponding to the second week of the

<sup>1</sup>CNRM/GMGEC/MEMO, Toulouse, Cédex 01, France.

<sup>2</sup>SHOM/CMO/BRESM, Toulouse, France.

<sup>3</sup>GRGS/LEGOS, Toulouse, France.

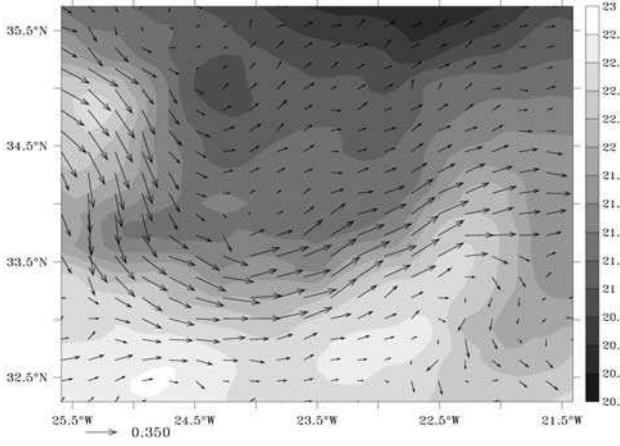


**Figure 1.** SST and current fields corresponding to the 20/10/93, beginning of the SEMAPHORE IOP. The arrow corresponds to  $0.35 \text{ ms}^{-1}$ .

SEMAPHORE IOP. All simulations started from 27/10/93 at 0h, standing for the unique, common, initial state. In the course of these simulations, different random perturbations were added to the reference wind field. Perturbations were obtained by the geostrophic relation from a set of Gaussian fields with a 500 km horizontal decorrelation scale and a one-day time decorrelation scale. These fields were calculated by the algorithm developed by Evensen [1994].

$$\mathbf{v}^i(x, y, t) = \mathbf{v}_{ref}(x, y, t) + \frac{g}{f} \mathbf{k} \times \mathcal{G}^i, \quad (1)$$

where,  $\mathbf{v}^i$  accounts for the  $i$ -th time-series of wind fields acting throughout the  $i$ -th simulation of the ensemble,  $\mathbf{v}_{ref}$  is the reference wind field,  $g$  gravity,  $\mathbf{k}$  the unitary vector at the local vertical.

[13] First and second order statistical moments have been calculated from the ensemble  $\{\mathbf{x}^i; i = 1, \dots, m\}$  of forecast states obtained through model integration. This yields an estimation of the system's *probability density function*, assuming this to be Gaussian:

$$\begin{aligned} \bar{\mathbf{x}}^e &= \frac{1}{m} \sum_{i=1}^m \mathbf{x}^i \\ \hat{\mathbf{P}}_e^f &= \langle \mathbf{x}^f, \mathbf{x}^f \rangle = \overline{(\mathbf{x}^f - \bar{\mathbf{x}}^e)(\mathbf{x}^f - \bar{\mathbf{x}}^e)^T}, \end{aligned} \quad (2)$$

[14] The ensemble mean,  $\bar{\mathbf{x}}^e$ , is considered as the best estimate of the ensemble forecast.  $\hat{\mathbf{P}}_e^f$  is an estimate of the forecast error covariance matrix  $\mathbf{P}^f$ . The diagonal elements of this matrix represent variance of the ensemble of forecast states with respect to their mean, reporting dispersion of the ensemble. In the present case, this corresponds to the error induced in model forecast by uncertainties in the forcing wind field, i.e. to the sensitivity to wind forcing errors.

[15] Mixed-layer heat-budget diagnostics have been estimated for each ensemble member via the formulation proposed by Caniaux and Planton [1998], that integrates the different terms contained in the prognostic equation for temperature, over the mixed-layer. Mixed-layer depth has

been diagnosed as the depth at which the vertical temperature gradient is equal to  $-0.05^\circ\text{C m}^{-1}$ .

#### 4. Results

[16] Dispersion about the ensemble mean forecast increases throughout integration, showing greatest temperature SDV about its mean at the end of 02/11/93 (seventh day of simulation).

[17] At the surface, model proves weak sensitivity to perturbations applied. SST SDV (Figure 2) shows a north-east-southwest pattern, with higher values at the east of the domain. More precisely, SDV exceeds  $0.15^\circ\text{C}$  in three distinct zones: in the north-eastern part of the domain, where it is maximum ( $0.2^\circ\text{C}$ ), and at two places located in the vicinity of the Azores Front. These secondary maxima ( $0.16^\circ\text{C}$  around  $34.7^\circ\text{N}, 25^\circ\text{W}$  and  $0.18^\circ\text{C}$  around  $33.4^\circ\text{N}, 21.6^\circ\text{W}$ ) occur over the mean SST front, precisely at the top of the meanders.

[18] When looking at the variability under the surface (at 52.5m, Figure 3), the pattern of maximum SDV is very different from that at the surface. Here the pattern is well correlated with the northern part of the Azores Front, meaning that the cold waters present in the domain are specially concerned with higher SDV. Moreover SDV reaches much higher values at 52.5 m depth than at the surface (larger than  $0.5^\circ\text{C}$  compared with  $0.2^\circ\text{C}$  peak values at the surface).

[19] A SDV cross section along  $21.85^\circ\text{W}$  containing the maximum of Figure 3, shows that the maximum SDV is not located in the mixed layer, but underneath (Figure 4a). This maximum, located near 60 m in the cold waters, overlaps the upper mean thermocline. Consequently, varying the amplitude of the wind forcing, results in a stronger variability not in the mixed layer but in the upper thermocline, and specially affects the cold waters at the north of the front.

[20] The stronger SDV in the upper thermocline (Figure 4) can be explained by variations of mixed-layer depth (MLD) about its mean. Indeed, strong fluctuations about strong forcing wind fields induce fluctuations of mixing within the mixed-layer and hence of thermocline erosion and entrainment at its bottom. Figure 4b shows a representative sample of temperature profiles at ( $34.63^\circ\text{N}, 21.85^\circ\text{W}$ ),

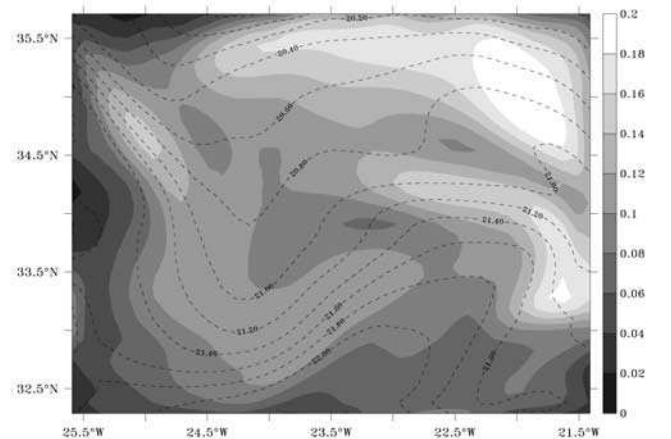


**Figure 2.** Ensemble mean (contour) and SDV (filled) of SST ( $^\circ\text{C}$ ) on 02/11/93 (end of simulation).

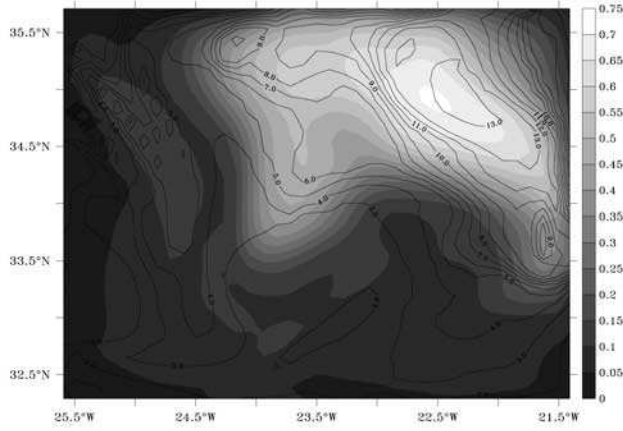


**Figure 3.** Variance of temperature ( $^{\circ}\text{C}$ ) at 52.5 m depth (filled pattern) and mixed-layer depth SDV contours (m) 02/11/93 (end of the simulation).

location for which a maximum of temperature SDV is found at 57.5m depth. Differences between ensemble member profiles and the mean temperature profile are homogeneous through the mixed-layer. These differences vary within the strong vertical temperature gradient, depending on mixed-layer depth and gradient steepness for each member profile, with respect to the ensemble mean profile. Figure 3 evinces good accordance of temperature SDV at 52.5 m depth and mixed-layer depth SDV.

[21] The horizontal pattern of SST SDV has been interpreted with the use of complementary diagnostics, namely the use of heat budget statistics over the ensemble. The peak of SST SDV (maximum of  $0.2^{\circ}\text{C}$  in Figure 2) in the north-eastern corner of the model, originates during 29/10/93, corresponding to the beginning of the storm. This storm remained quite stationary during 29/10/93 to 31/10/93 at the east of the domain, consequently generating strong north-westerly winds during all this period. In this area, fluctuations in horizontal advection are combined with stronger heat flux dispersion (Figure 5b) and entrainment through the mixed layer (not shown). The combined action of these

three- and one-dimensional processes has a strong impact on mixed layer thermal content.

[22] As established by *Caniaux and Planton* [1998], horizontal advection is locally one of the main processes accounting for the mixed-layer heat budget during the SEMAPHORE IOP. Horizontal advection exhibits high SDV values that can exceed  $200 \text{ W/m}^2$ , about our ensemble mean (Figure 5a). This is the case for 29/10/93, 30/10/93 and 31/10/93, corresponding to wind enhancement due to the influence of the storm. The persistence of strong north-westerly winds during three days, resulted in important Ekman drift, acting south-westwards and contributing to isotherm horizontal displacement at precise spots of the meander of the Azores Front. Variations in wind speed and direction produced by perturbations then result in modifications of the advective response of the model, which will be most notable in regions of sharp, parallel-to-the-mean-wind, SST gradients. In our case, at the crest of the two meanders of the Azores Front present at  $34.7^{\circ}\text{N}, 25^{\circ}\text{W}$  and at  $33.4^{\circ}\text{N}, 21.6^{\circ}\text{W}$ . Figure 5a shows the coincidence of both horizontal advection and SST SDV on the third day of simulation (29/10/93). This result indicates that not only local, one dimensional processes are active on the domain in response to the variability of fluxes, but that there is also a three dimensional response of the oceanic upper layers. This response is associated to the frontal structure in the temperature (and salinity) fields.

## 5. Conclusions

[23] Monte Carlo simulations have been run on a primitive equation open-ocean model to assess the impact of wind-induced errors in air-sea fluxes upon model forecast. This method is particularly well suited to investigate where the response of the upper ocean is affected by surface fluxes. Combined with diagnostics in the mixed layer, this method is a powerful tool to understand the active physical processes. Moreover, it provides the possibility of evaluating model forecast errors when no validating data sets are available.

[24] The computation of mixed-layer heat budgets for every ensemble member has provided detailed information

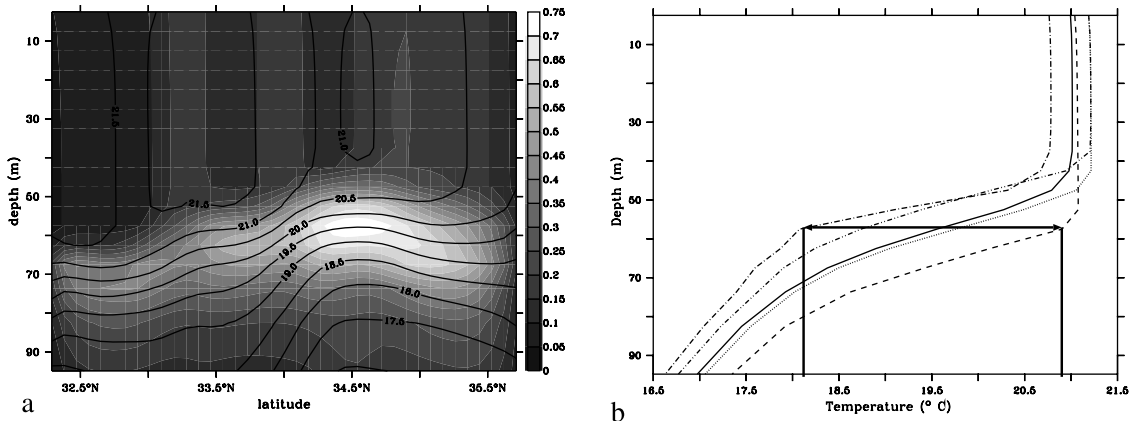


**Figure 4.** Vertical slice of temperature mean and SDV (both in  $^{\circ}\text{C}$ ) at  $21.85^{\circ}\text{W}$ , where ensemble dispersion is maximum (a). Figure (b) shows a sample of vertical profiles representative of the ensemble dispersion at point ( $34.63^{\circ}\text{N}, 21.85^{\circ}\text{W}$ ), contained in the section. These profiles illustrate the fact that greater SDV in subsurface is associated to vertical displacement of mixed-layer bottom.



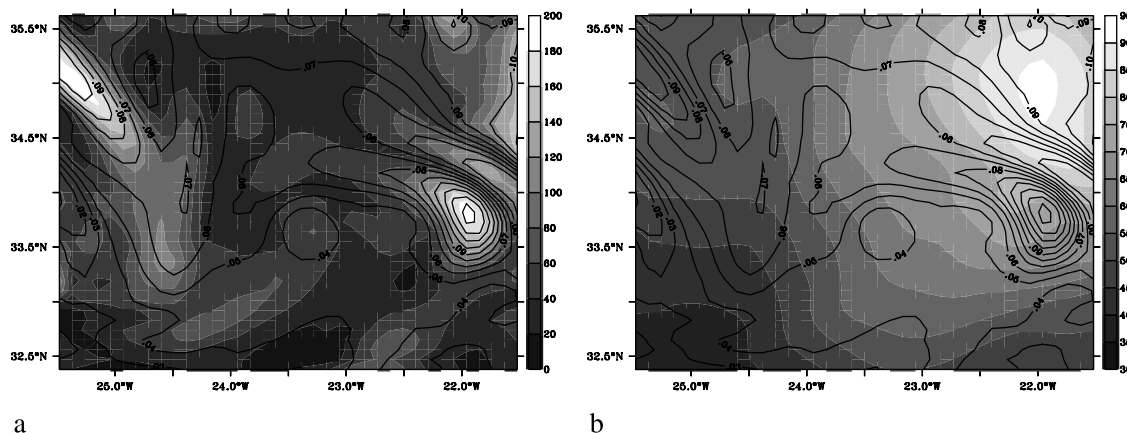


**Figure 5.** Standard-deviation of the horizontal advection ( $W/m^2$ ) averaged over 29/10/93 (a). Standard-deviation of the total surface heat flux averaged over 29/10/93 ( $W/m^2$ ) of simulation (b). Overlaid contours show SST SDV ( $^{\circ}C$ ) on 29/10/93 at 24<sup>h</sup> (on both figures).

about the one- and three-dimensional processes responsible for forecast error growth in this region, marked by the presence of the Azores frontal system.

[25] Dispersion of the thermal field about its ensemble mean, has shown that the strongest sensitivity of the model is located at the top of the ensemble-mean thermocline. The rather weak sensitivity of surface temperature to perturbations in air-sea heat and momentum fluxes is due to the fact that the initial state from which the ensemble has been run, consists of a well developed mixed-layer ocean, undergoing strong wind episodes and decreasing insolation during the mixed-layer deepening season. In this context, strong amplitude perturbations of the wind field are mostly perceived at the top of the thermocline, as a consequence of fluctuations in mixing and entrainment processes within and into the mixed-layer.

[26] Horizontal structure of temperature SDV down the mixed-layer is mostly accounted for by advective processes related to Ekman drift, specially marked over the tighter frontal temperature gradients. Nevertheless, surface heat fluxes can have a local impact on model's thermal response that extends down the whole mixed-layer through vertical processes. Entrainment through the mixed layer base also contributes to the horizontal pattern of temperature SDV.

[27] Matrix  $\hat{P}_e^f$  provides an estimation of model error covariance matrix. Examining other elements of this matrix would let us detect the response of other variables characterizing the state of the system, for example the sensitivity of ocean current to perturbations applied, or the simultaneous response of temperature and salinity to these perturbations. Furthermore, following the representer approach [Bennett, 1992], matrix  $\hat{P}_e^f$  can be used to assess the correction provided by a single observation onto the model forecast state. This approach has been followed by Echevin et al. [2000] to evaluate the impact of sea level observations on model state variables. This framework permits the evaluation of different types of observations, in situ or satellite, and is actually being used to study the impact of SST assimilation in the model presented in this paper.

[28] **Acknowledgments.** Authors wish to thank Dr. Geir Evensen and Dr. Vincent Echevin for their help with ensembles.

[29] This study has been carried out with the financial support of the SHOM (Service Hydrographique et Océanique de la Marine, France) and CNRM (Centre National de Recherches Météorologiques, Toulouse, France).

## References

- Bennett, A. F., *Inverse Methods in Physical Oceanography*, Cambridge University Press, 346 pp., 1992.
- Caniaux, G., and S. Planton, A three-dimensional ocean mesoscale simulation using data from the SEMAPHORE experiment: Mixed layer heat budget, *J. Geophys. Res.*, 103(C11), 25,081–25,099, 1998.
- Echevin, V., P. De Mey, and G. Evensen, Horizontal and Vertical Structure of the Representer Functions for Sea Surface Measurements in a Coastal Circulation Model, *J. Geophys. Res.*, 30, 2627–2635, 2000.
- Evensen, G., Sequential data assimilation with a nonlinear quasi-geostrophic model using Monte Carlo methods to forecast error statistics, *J. Geophys. Res.*, 99(C5), 10,143–10,162, 1994.
- Eymard, L., et al., Study of the air-sea interactions at the mesoscale: the SEMAPHORE experiment, *Annales Geophysicae*, 14, 986–1015, 1997.
- Fairall, C. W., J. E. Hare, E. F. Bradley, A. A. Gratchev, and J. B. Edson, Preliminary results from the ETL open ocean air-sea flux database, in *Extended abstracts from the WCRP/SCOR Workshop on Inter-comparison and validation of ocean-atmosphere flux fields*, Washington DC, 21–24 May, in press, 2001.
- Gavart, M., P. De Mey, and G. Caniaux, Assimilation of satellite altimeter data in a primitive-equation model of the Azores-Madeira region, *dynamics of atmospheres and oceans*, 29, 217–254, 1999.
- Larsen, S. E., et al., AUTOFLUX: An autonomous flux-package for measuring the air-sea flux momentum, heat, water-vapor and carbon dioxide, in *Proceeding of EUROCEAN 2000 conference*, Hamburg, Germany, 29 August–2 September 2000.
- Large, W. G., and S. Pond, Open ocean momentum flux measurements in moderate to strong winds, *J. Phys. Oceanogr.*, 11, 324–336, 1981.
- Large, W. G., and S. Pond, Sensible and latent heat flux measurements over the ocean, *J. Phys. Oceanogr.*, 12, 464–482, 1982.
- Madec, G., P. Delecluse, M. Imbard, and C. Levy, OPA, release 8, Ocean General Circulation Model reference Manual, LODYC/IPSL, France, internal report 96/xx, February 1997.
- Weill, A., et al., Toward a better determination of turbulent air-sea fluxes from several experiments, accepted in *J. Clim.*, 2002.
- I. A. Burillo, CNRM/GMGEC/MEMO, Météo-France, 42, avenue G. Coriolis, Toulouse, 31057 Cédex 01, France. (Isabel.Andreu-Burillo@meteo.fr)
- G. Caniaux, CNRM/GMGEC/MEMO, Météo-France, 42, avenue G. Coriolis, Toulouse, 31057 Cédex 01, France. (Guy.Caniaux@meteo.fr)
- M. Gavart, SHOM/CMO/BRESM, 14, avenue E. Belin, Toulouse, 31400, France. (gavart@cnes.fr)
- P. De Mey, GRGS/LEGOS, 18, avenue E. Belin, Toulouse, 31401, France. (Pierre.De-Mey@cnes.fr)
- R. Baraille, SHOM/CMO/BRESM, 14, avenue E. Belin, Toulouse, 31400, France. (baraille@cnes.fr)